Stretching-Induced Growth of PEDOT-Rich Cores: A New Mechanism for Strain-Dependent Resistivity Change in PEDOT:PSS Films

Yoo-Yong Lee, Ji-Hoon Lee, Ju-Young Cho, Na-Rae Kim, Dae-Hyun Nam, In-Suk Choi, Ki Tae Nam,* and Young-Chang Joo**

It remains a fundamental challenge in the development of stretchable electronics to understand how mechanical strain changes the electrical properties of materials. Although the piezoresistive behavior of poly(3,4-ethylenedioxythiophene):poly(styrenesulfonate) (PEDOT:PSS) has been observed, its intrinsic origin is not yet fully understood because there are many extrinsic contributing factors and an experimental platform with which to assess such behavior has not been established. Here, systematic analysis shows that the matching Poisson's ratio and elastic modulus between PEDOT:PSS films and their underlying substrates is important in decoupling the factors that affect the material's piezoresistivity, allowing for tunable resistivity. Based on such a fundamental understanding, the conductivity of PEDOT:PSS can be controlled to be invariant and decrease as a function of applied tensile stress. Furthermore, a linear response of the resistivity with respect to mechanical strains of up to 60%, which has never before been realized, is shown. The irreversible conductivity enhancement is primarily caused by the coalescence-induced growth of conductive PEDOT-rich cores.

1. Introduction

The electrical conductivity of materials generally decreases under mechanical deformation. However, in several materials, such as n-doped silicon, the mobility can be enhanced under tensile strain because of a change in the materials' electronic band structure.[1] This change in conductivity, which is an intrinsic material property, is valid only within the elastic strain region, whereas under huge deformations, extrinsic factors such as the generation of defects,[2–4] microstructural and dimensional changes,[5,6] and neighboring materials[7–9] can influence the conductivity in concerted ways. For stretchable electronics in particular, these factors should be controlled and restrained to develop conductors or interconnects that endure high applied strain. Previous approaches to overcoming this challenge for stretchable conductors can be categorized into two types of methods. The first is the hybridization of metallic and organic materials that can withstand large strains without rupturing.[10–12] The second is the design of structures, such as wavy-, net-, or arc-shaped conductors, that can undergo larger strains than plane-shaped structures due to their ability to be stretched.[13–15] To develop further improvements, understanding the mechanism governing the change in electrical properties and decoupling the contribution of each influencing factor are highly important. In this study, we chose the conducting polymer poly(3,4-ethylenedioxythiophene):poly(styrenesulfonate) (PEDOT:PSS) to produce films that have innate flexibility under mechanical strain. The resistivity response of PEDOT:PSS films to an applied tensile strain was directly investigated, and the key parameters that control the strain-response behavior were identified. By selecting mechanically suitable substrates for the PEDOT:PSS films, each factor that influences the resistance change in a complex manner was distinguished. Moreover, we demonstrated that the resistivity of the films can be modulated, which may be useful in developing conducting polymer electrodes for stretchable electronics.

The conductivity of as-deposited pristine PEDOT:PSS films is approximately <1 S cm^{-1}, but it can be improved by controlling the PEDOT-to-PSS ratio,[16] UV radiation,[17] thermal treatment,[18] or, more dramatically, by secondary doping with the addition of solvents.[18–24] Although previous data have shown that the conductivity of such films also depends on the applied strain, there is no consistency between the range of values over which the resistance changes and the mechanisms that have been proposed for this change. The relative change in the resistance under elastic strain, which is known as the gauge factor, has been reported to be 5.2 and 17.8, indicating positive piezoresistivity.[25,26] It should be noted that these measurements were performed using the bending strain test with applied strains of less than 1%. In contrast, several previous studies have shown

Y.-Y. Lee, J.-H. Lee, J.-Y. Cho, N.-R. Kim, D.-H. Nam, Prof. K. T. Nam, Prof. Y.-C. Joo
Department of Materials Science and Engineering
Seoul National University
Seoul, 151-744, Republic of Korea
E-mail: nkitae@snu.ac.kr; ycjoo@snu.ac.kr
Dr. I.-S. Choi
High Temperature Energy Materials Research Center
Korea Institute of Science and Technology (KIST)
Seoul, 136-791, Republic of Korea
E-mail: insukchoi@kist.re.kr

DOI: 10.1002/adfm.201203670

that the resistivity decreases by 15% when small and finite tensile strains of less than 10% are applied.[27,28] However, the continuous increase in the tensile strain ultimately resulted in an abrupt increase in the resistance due to the cracking of the films. These changes in resistance are associated with different complex factors that originate from not only a change in intrinsic properties with strain but also from extrinsic factors, such as dimensional changes and the generation of defects in the films. Additionally, there are no previous reports regarding the observation of resistance changes at large strains greater than 30% due to the cracking of PEDOT:PSS films or the rupturing of the underlying substrates.

In this study, we successfully investigated the change in the resistivity of PEDOT:PSS films up to strains of 60% by matching the Poisson's ratio and elastic modulus between the substrates and the films and decoupled the changes into several underlying mechanisms. We then demonstrated how the resistivity can be modulated under mechanical strain from invariant values to "decreasing" values up to 90%. Surprisingly, the irreversible growth of conductive PEDOT-rich cores is the primary mechanism for the enhancement of conductivity purely induced by applied strain.

2. Results and Discussion

2.1. Effects of Substrates on Resistance Changes Under Large Strain

In principle, the origins of extrinsic resistance changes in PEDOT:PSS films deposited on compliant substrates under tensile conditions can be divided into the following two major contributions. The first contribution is the change in the geometrical shape of PEDOT:PSS films resulting from tensile deformation. When a substrate is stretched along a longitudinal direction, the length (l) of the supported film increases but the width (w) and thickness (t) decrease. Given that the resistivity (ρ) is constant under tensile deformation, the variation in resistance ($\Delta R_G/R_0$) induced by the geometric change can be described by Equation (1):

$$\frac{\Delta R_G}{R_0} = \frac{R_G - R_0}{R_0} = \left[\frac{l/l_0}{(w/w_0)(t/t_0)} - 1\right] \quad (1)$$

where l/l_0 is the extension ratio of the film and w/w_0 and t/t_0 denote the contraction ratio of the width and the thickness, respectively. The above equation predicts that the resistance always increases as a result of such a geometrical change during tensile deformation.

The second contribution is the generation of defects (buckles and cracks) in PEDOT:PSS films. Generally, when a large strain (>10%) is applied, this mechanism becomes dominent, which results in an abrupt increase in electrical resistance. The cracks normally can form in the films with applied strain for free standing states and fractured at a small strain. However, the formation of the defects can be suppressed when the PEDOT:PSS film is deposited to a compliant substrate. Furthermore, the abrupt fracture of the film can be retarded at even higher strain by matching the elastic modulus and Poisson's ratio between the film and the substrate. For example, poly(dimethylsiloxane) (PDMS) is conventionally used as a substrate for stretchable devices. However, the Poisson's ratio, elastic modulus, and elastic strain limit of PDMS are quite different from those of PEDOT:PSS, as listed in **Table 1**.[29,30] Such huge differences in mechanical properties result in a local instability at the interface, which generates cracks in the films during stretching. For example, in a previous experiment, cracks started to form at 12% strain and the resistance increased abruptly at approximately 30% strain as a result of the accumulation of cracks.[27] Moreover, the treatment of PDMS with O_2 plasma or UV/O_3 to activate the surface generates thin SiO_x layers,[31–33] which leads to the brittle facture of the films, even at extremely low strains. It seems that the abrupt and irreversible increase in resistance is inevitable after stretching and releasing PEDOT:PSS deposited on PDMS.

Table 1. The mechanical properties of PEDOT:PSS, PDMS, and PI films.

	PEDOT:PSS[29]	PDMS[30]	PI[34]
Poisson's ratio	0.34–0.35	0.5	0.34
Elastic modulus (MPa)	2000	0.1–3	3200
Elastic strain limit (%)	2	≈160	2

To eliminate or minimize the effects of defects, we chose polyimide (PI) as a substrate material instead of PDMS. As shown in Table 1, the Poisson's ratio and elastic strain limit of PI are exactly the same as those of PEDOT:PSS (0.35 and 2%, respectively), and the materials' elastic modulus are also similar.[29,34] Thus, we expect that using a PI substrate would allow us to observe the intrinsic behavior of PEDOT:PSS by preventing the generation of cracks or buckles.

To examine the effects induced by substrate type, PEDOT:PSS films were deposited on PI substrates and PDMS substrates. The change in the electrical resistance of the PEDOT:PSS films on the PDMS and PI substrates with tensile strain was investigated using the in situ resistance measurement tensile test system schematically shown in **Figure 1**. The strain of the samples was monitored by optically measuring the distance between markers on the samples. The relative resistance changes ($(R–R_0)/R_0$ (%)) in PEDOT:PSS films doped with 5 wt% dimethyl sulfoxide (DMSO) on PI and PDMS substrates with tensile strain are shown in **Figure 2** as the representative cases. In the case of the PDMS substrate, an abrupt increase in resistance was observed at small tensile strain (<3%). The formation of cracks in the film is responsible for such a rapid increase in resistance in the film because it facilitates the local delamination of the films, as indicated by the in situ observation of the film surfaces by microscopy during stretching and releasing (**Figure 3**a). When the Poisson's ratio of the substrates is larger than that of the films, a compressive force perpendicular to the stretching direction is exerted on the films during stretching. This leads to the formation of dense lateral buckles on the surface. These dense buckles at the interface induce instabilities in local adhesion, and cracking subsequently occurs perpendicular to the stretching direction. These cracks are permanent defects and do not disappear after deformation. Furthermore, the

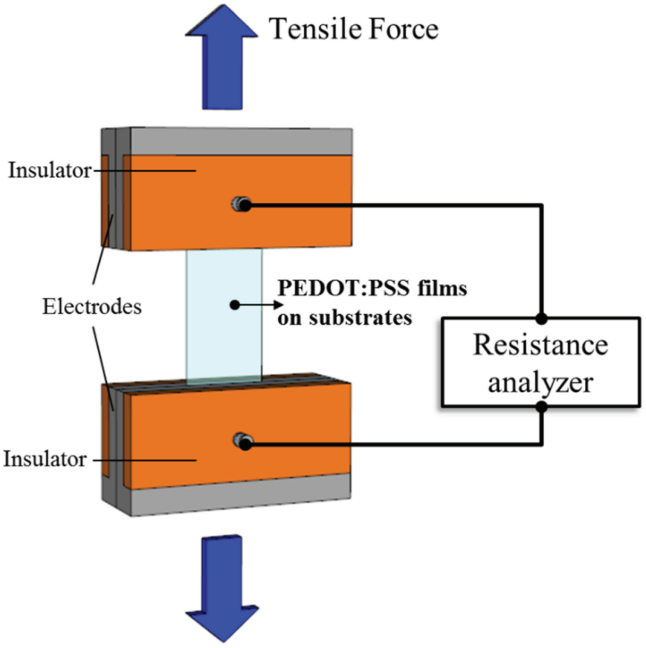

Figure 1. Experimental set-up for the in situ measurement of the electrical resistance of PEDOT:PSS films during the tensile stretching of the films coated on PI or PDMS substrates.

elastic strain limit of PEDOT:PSS is approximately 2%; therefore, plastic deformation occurs in PEDOT:PSS at these strains. As the substrates were released, the lateral buckles disappeared, but vertical buckles formed due to the previous plastic deformation of the PEDOT:PSS film. The in situ morphologies of the films during this process are shown in greater detail in Figure S1.

A completely different behavior was observed for the PI substrates. The change in the resistance of the films increased gradually with strain, and we could successfully stretch the film up

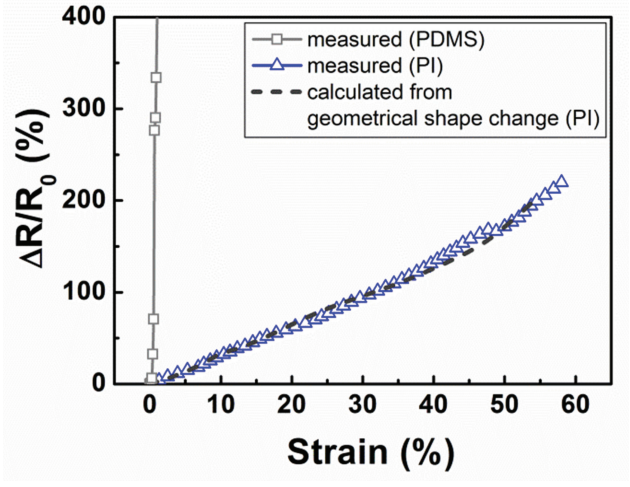

Figure 2. Relative resistance change ($\Delta R/R_0$ (%)) of PEDOT:PSS films doped with 5 wt% DMSO as a function of tensile strain of PDMS and PI substrates. For comparison, the resistance changes calculated from the change in the geometry of the PI substrates are presented as dotted lines.

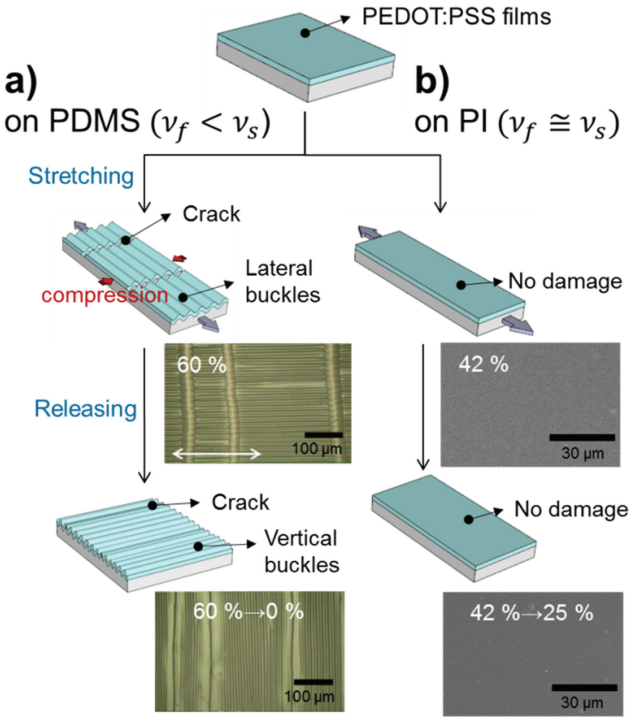

Figure 3. Schematics and optical/SEM images of PEDOT:PSS films on PDMS and PI substrates during substrate stretching according to the difference in the Poisson's ratio between the films and the substrates at a) $\nu_f < \nu_s$ and b) $\nu_f \cong \nu_s$, where ν_f and ν_s are the Poisson's ratios of the films and the substrates, respectively. The stretching direction is indicated by arrows in the microscopy images.

to 60% strain without generating buckles or cracks. No damage was observed on the surface of the PEDOT:PSS films deposited on the PI substrates during or after the stretching of the sample up to 60% strain (Figure 3b and Supporting Information Figure S1). The Poisson's ratio of the films is similar to that of the substrates; therefore, the films and the substrates are uniformly deformed and experience the same Poisson's compression perpendicular to the stretching direction. Tensile testing was terminated at 60% strain due to the rupture of the substrate. To our knowledge, a gradual increase in resistance at strains of up to 60% has never been observed before in PEDOT:PSS films. Because the PI substrate allowed the PEDOT:PSS films to remain crack-free up to 60% strain, we believe that the intrinsic behavior of the films could be observed.

The gradual increase in the resistance of the PEDOT:PSS films on the PI substrates is completely attributed to the change in the geometry ($\Delta R_G/R_0$) of the films during tensile testing, as formulated in Equation (1). We plotted ($\Delta R_G/R_0$) in Figure 2, where the extension in the length and contraction in the width were optically measured by monitoring a marker's movement on the substrates. The contraction in thickness can be calculated, assuming that the film undergoes Poisson's compression, $(1 - \nu_f\varepsilon_l)$, where ν_f is the Poisson's ratio of PEDOT:PSS (0.35) and ε_l is longitudinal strain. The measured resistance change matches well with the expected increase due to a change in geometry, which confirms that there was no contribution from cracking when using the PI substrates.

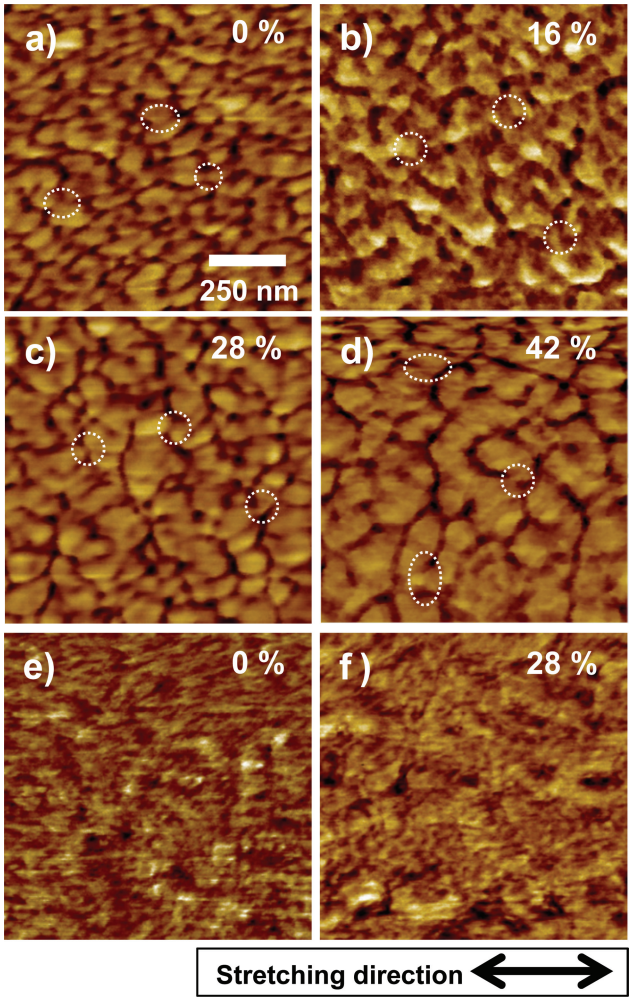

Figure 4. AFM phase images of a–d) pristine and e,f) 5 wt% DMSO-doped PEDOT:PSS films at each strain denoted in the images. The arrow indicates the stretching direction and all images were obtained using tapping-mode AFM at a scale of 1×1 μm^2.

Because the two major extrinsic contributions to the resistance change were eliminated, we could identify the purely intrinsic factors affecting the change in resistance by in-situ electrical measurements conducted over a wide range of deformation states, from small elastic strain to 60% strain.

2.2. Change in Electrical Resistivity of PEDOT:PSS with Mechanical Strain

After we confirmed that PI substrates are suitable in providing a crack-free condition, we investigated how the doping of PEDOT:PSS films with DMSO affects the strain-resistance response. It is well known that secondary doping with DMSO can enhance the conductivity of PEDOT:PSS by about three orders of magnitude. The initial morphology of pristine PEDOT:PSS (**Figure 4**a) consists of conductive and tangled PEDOT-rich cores (bright regions in the images) surrounded by insulating shells composed of excess PSS chains (dark region in the images).[21,35] The conductivity is very low (<1 S cm^{-1}) because the PSS shells serve as barriers to charge transport. However, when doped with DMSO (Figure 4e), the cores and the insulating shells were wholly dissolved. According to previous studies, the main effect of doping is the transformation of the PEODT chains' coiled conformation into a linear one and the homogeneous dispersion of the cores.[23,36–38] This morphological change enhances the connectivity of the individual PEDOT chains, and the resulting enhancement increases the conductivity. Our question was how such a difference in morphology induced by DMSO doping affects the resistance change responding to the large applied strain.

We investigated the relative resistance changes of PEDOT:PSS films doped with 0, 5, and 10 wt% DMSO as a function of strain, which are shown in **Figure 5**a. Pristine PEDOT:PSS films (0 wt% DMSO) and DMSO-doped films (5 and 10 wt%) exhibited completely opposite resistance responses to the applied strain. While the resistance increases with strain in the case of the DMSO-doped PEDOT:PSS, it decreases in the pristine film. This increasing and decreasing trend continues up to 60% strain. The positive dependence of resistance on strain has been observed under many experimental conditions, regardless of the doping conditions. However, the negative dependence observed in the pristine film has never been observed before in PEDOT:PSS subject to such large strains. A previous study reported the observation of this negative dependence along the stretched direction only below 10% strain.[28] When the strain increased above 10%, the resistance abruptly increased due to the generation of cracks, and the films ultimately ruptured. Becuase the formation of cracks were effectevly retarded at the interface by using PI substrates, the observed strain dependence resulted only from the change in the geometry and the intrinsic properties of the films, i.e., the morphological transformation of the pristine PEDOT:PSS films with strain.

To determine the purely intrinsic resistivity change, the geometric contribution was calculated and subtracted from the measured resistance. The relationship between the relative resistance and the resistivity change can be expressed by Equation (2):

$$\frac{R}{R_0} = \frac{\Delta R}{R_0} + 1 = \frac{\rho}{\rho_0}\left[\frac{l/l_0}{(w/w_0)\left(1 - v_f \varepsilon_l\right)}\right] = \frac{\rho}{\rho_0}\left[\frac{\Delta R_G}{R_0} + 1\right] \quad (2)$$

where $\Delta R/R_0$ and $\Delta R_G/R_0$ are the normalized change in the measured resistance and that induced by a change in geometry, respectively. The equation can be rearranged to obtain the resistivity of the PEDOT:PSS films at each strain:

$$\rho = \rho_0\left[\frac{\Delta R}{R_0} + 1\right] \Big/ \left[\frac{\Delta R_G}{R_0} + 1\right] \quad (3)$$

The values of $\Delta R/R_0$ and $\Delta R_G/R_0$ were obtained from Figure 5a. The resistivity is plotted as a function of the strain of the films in Figure 5b. The resistivity of the DMSO-doped films was invariant as a function of strain. On the other hand, interestingly, the resistivity of the pristine films gradually decreased as the strain increased. When we examined

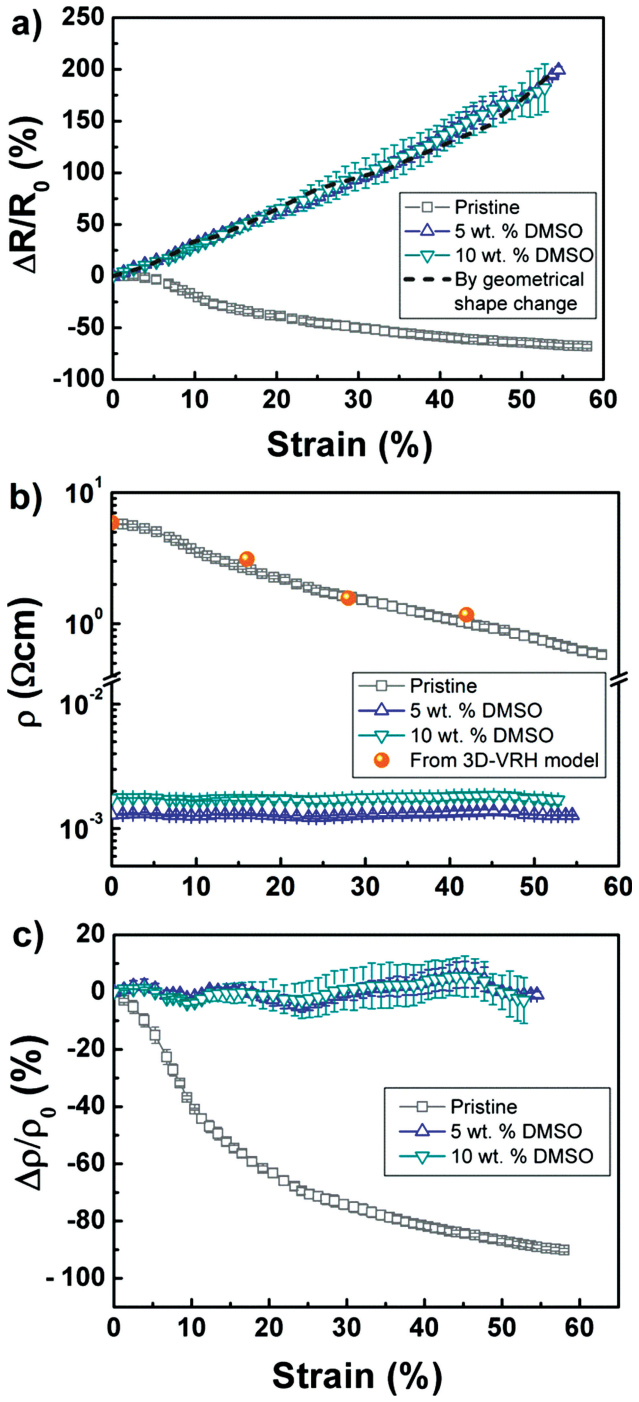

Figure 5. a) Relative resistance change of PEDOT:PSS films doped with various concentrations of DMSO (0, 5, and 10 wt%) on O_2-plasma-treated PI substrates during stretching to up to 60% strain. b) The resistivity and c) relative change in resistivity of PEDOT:PSS films as a function of strain. The orange spheres denote the resistivities calculated from the 3D VRH model.

the relative change in the resistivity, shown in Figure 5c, the change in the DMSO-doped films was observed to remain constant and only fluctuated by approximately 10% at maximum. However, the resistivity of the pristine films decreased by 90% at a strain of 60%. These changes are only caused by the morphological change of the PEDOT:PSS films induced by strain. This suggests that the change in resistivity can be modulated from invariant to negative values by controlling not only the DMSO doping conditions but also the mechanical strain. Now, we discuss the mechanism governing the change in resistivity, focusing on the correlation between the change in morphology and the film strain.

2.3. Morphological Change Induced by Tensile Deformation

To investigate the difference in the resistivity-strain response between 5 wt% DMSO-doped and pristine PEDOT:PSS films, the morphological change of the films with tensile strain was investigated using AFM phase images (Figure 4). Comparing the initial morphology (Figure 4e) with the morphology of the DMSO-doped films after being strained 28% (Figure 4f), no significant changes were observed. This result indicates that the connectivity between the PEDOT chains was not significantly degraded with respect to the tensile deformation because the initial morphology already showed fully delocalized and uniformly dispersed PEDOT chains. Hence, no changes in the resistivity were observed as a function of strain.

By contrast, for the pristine PEDOT:PSS films, the size of the PEDOT-rich cores increased and the number of PSS barriers decreased as the strain increased (Figure 4a–d). Image analysis provides more quantitative information regarding the increase in the surface area of the PEDOT-rich cores. In those AFM phase images, the scanned area is 1 μm × 1 μm. The average surface area of the cores increased to 0.88, 1.27, 2.00, and 2.50×10^{-2} μm for strains of 0, 16, 28, and 42%, respectively. The detail information is presented in Supporting Information Figure S2 and S3. Compared with the initial core size, the average size increased by more than 185%. Such large growth of the PEDOT-rich cores is unexpected and cannot be explained by core elongation due to tensile stress. For example, in the 42% strained film, if a single core is considered, the extension along the applied strain direction will be 42% and the contraction perpendicular to the strain direction will be 18%. This calculation indicates that the increase in surface area should be 16%, which is much smaller than our measured value (185%). Therefore, our analysis shows that core coalescence or agglomeration results in apparent core growth. Additional evidence shows that the cores were grown not only parallel but also perpendicular to the direction of tensile strain, as shown in Figure 4a–d.

To understand the effect of core coalescence, we took a close look at the boundaries between the PEDOT cores neighboring the PSS shells. As indicated by the dotted white circles, the PEDOT-rich cores were not fully enclosed by the PSS shells. The non-uniform contrast in the phase image indicates a variation in the local density. The PSS shells (dark brown) have different thicknesses and are not fully connected. It should be noted that the multiple PEDOT-rich cores are connected in a lasagna-like structure. It is that such morphology can be formed favorably during thermal treatment when the film is deposited by spin coating.[39] In this structure, gel particles of PEDOT:PSS in the solution are shirked along the lateral and perpendicular direction, which results in the lasagna-like

structure. Approximately 5–10% of the circumference of the PEDOT cores is open to the neighboring cores, and the width of the connected channel is approximately 20 nm. The direction of the open sites is isotropic, and the number of sites per core is not uniform. In our AFM analysis, our observation was limited to the in-plane surface such that only two-dimensional connectivity could be observed. Because the spherical PEDOT-rich cores are wrapped three-dimensionally by PSS domains, the actual three-dimensional connectivity should be larger than that indicated by our observation. We believe that the PEDOT-rich cores start to coalesce together when the PEDOT chains are transported through the connected channels.

Our observation is the first demonstration of mechanically induced annealing for the growth of PEDOT-rich cores. It is known that thermal annealing can increase the size of cores. A previous study showed that when a PEDOT:PSS film was annealed from 100 °C to 200 °C, the growth of PEDOT-rich cores could observed by the coalescence of the cores.[18] However, there has been no prior observation of core growth induced by stretching. Energetically, a deformed system subject to excessive strain tends to minimize the strain energy. In case of the crack-free PEDOT-PSS films, large amount of applied strain cannot be relieved through the crack generation. The morphological transformation can be an alternative way to relieve the strain energy. Hence, in this study, the driving force of mechanical annealing should be the strain energy developed in the PEDOT:PSS films due to the large extent of deformation. Because the elastic modulus of the PEDOT-rich cores is theoretically lower than that of the PSS-rich shells,[40] the cores possibly develop a lower strain energy than that of the PSS-rich shells upon straining. Hence, the growth of PEDOT-rich cores is energetically favorable. Furthermore, the coalescence of the PEDOT-rich cores leads to an increase in configurational entropy in the core, which may also reduce the elastic modulus. However, the exact mechanism that explains how PEDOT-rich core growth minimizes the strain energy in films is still not clear; thus, further studies should be performed.

2.4. Resistance Change Due to the Coalescence of Cores in Pristine PEDOT:PSS

The decrease in the resistivity of pristine PEDOT:PSS films was quantified from the size of conductive PEDOT-rich cores. Charge transport in PEDOT:PSS films can be modeled by a variable range hopping (VRH) process.[41] Generally, the VRH model theorized the conduction in strongly disordered systems, which consist of insulating barriers and conducting region with localized states.[42] In VRH, the resistivity (ρ) of the films is expressed by,

$$\rho = \rho_0 \exp\left[\left(\frac{T_0}{T}\right)\right]^{\alpha} \quad (4)$$

where ρ_0 is the resistivity at infinite temperature and exponent α is equal to $1/(1 + D)$ related to the signature of VRH in D dimensions. In the case of pristine PEDOT:PSS films, we used 3D VRH model for lateral charge hopping and the exponent α becomes ¼.[41] T_0 is a material-dependent parameter represented by $T_0 = \beta/k_B N(E_F)\xi^3$, where ξ is the localization length, β is a numerical factor, k_B is the Boltzmann constant, and $N(E_F)$ is the density of states at the Fermi level. Among these parameters, the localization length, ξ, should be closely related to the dimensions of PEDOT-rich cores and can be expressed by $\xi = ad/s$, where a, d and s are the tunneling decay length in the barriers, the core diameter and the barrier thickness, respectively. Therefore, an increase in core size leads to an increase in the localization length of PEDOT:PSS films, which in turn leads to an enhancement in charge transport.

We then switched the change in the resistivity with the initial resistivity and the diameter of the cores before and after deformation at the same temperature by dividing Equation (4).

$$\rho^* = \rho\left(\frac{\rho}{\rho_0}\right)^{\left[\left(\frac{d^*s}{ds^*}\right)^{-\frac{3}{4}}-1\right]} \quad (5)$$

where ρ and ρ^* are the initial and the final resistivities and d^* and s^* are the core diameter and the barrier thickness after deformation, respectively. The cores diameters are 52, 64, 80, and 89 nm for strains of 0%, 16%, 28%, and 42%, respectively. We obtained these values from each area of the cores by assuming that these cores were circular in shape and that the PSS shell thickness and tunneling decay length were constant. By substituting the measured core diameters into the equation above, the resistivity at each strain of the films was plotted in Figure 5b as an orange shperes. These values match the experimental data quite well. Therefore, the growth in core size directly results in an increase in the localization length in a VRH process.

2.5. Characteristics of the Resistivity Change Induced by Morphology Under Large Strain

The resistivity change induced by the growth of PEDOT-rich cores under large strain is characteristically different from changes induced by elastic deformation under small strain. **Figure 6** shows the change in the resistivity of the PEDOT:PSS films on PI substrates during stretching/releasing cycles as well as the anisotropic change in resistivity (resistivity parallel vs. perpendicular to the stretching direction of the films).

Figure 6a shows that the resistivity of the 5 wt% DMSO-doped films did not change upon stretching and releasing the films, as expected. However, the pristine PEDOT:PSS films showed different behavior depending on the applied strain. First, the films were stretched and released under a small strain (less than 10%); the resistivity recovered reversibly to the released strain. (Figure 6a). In the strain region between 2% and 10%, the plastic deformation of the film occurred so that the film dimension was not fully recovered to the initial even after the releasing. Because of the plastic deformation, the resistivity was not also fully recovered to the initial value but returned to the value at the load-free state (4.6% strain). Interestingly, during the releasing, the resistivity change returned by following the path obtained during the stretching as shown in Figure 6a. However, for large deformation (above 17% strain), the resistivity decreased permanently and was not recovered upon releasing. Due to the plastic deformation of the PEDOT:PSS films and PI substrates, the samples were not recovered to the initial dimension after the releasing.

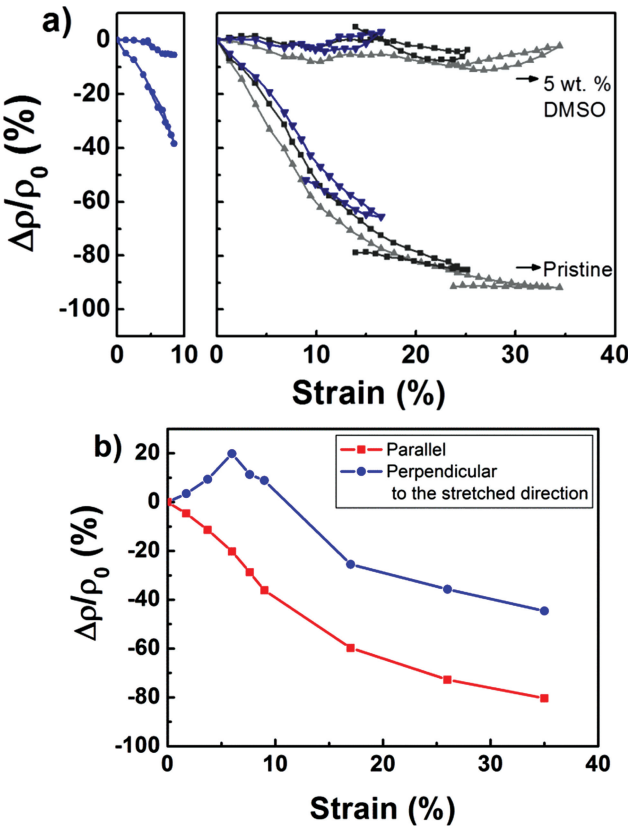

Figure 6. a) Relative resistivity change ($\Delta\rho/\rho_0$(%)). of PEDOT:PSS films as a function of strain (9, 17, 26, and 35%) for the pristine and 5 wt% DMSO-doped films. b) The change in the resistivity parallel and perpendicular to the stretching direction of the pristine films.

Furthermore, Figure 6b shows that the resistivity parallel and perpendicular to the stretching direction. Upon stretching, the resistivity decreased along the parallel direction but increased along the perpendicular direction. Such anisotropy was maintained up to a strain of 7%; however, under larger deformation, above 7% strain, it disappeared. This anisotropic change and the recovery of the resistivity in the small-strain region (<10%) are caused by the elastic recovery of the single PEDOT-rich cores. The conductivity of the stretched conductive polymer may have been enhanced by a few possible mechanisms, such as an increase in inter-chain conductivity due to alignment and an increase in the degree of crystallinity.[43,44] Regardless of the mechanism, the anisotropic change in resistivity has also been reported.[28] During stretching, the diameter of the PEODT-rich cores increased parallel to the stretching direction, which enhanced the conductivity along that direction. However, charge transport was retarded in the perpendicular direction because the core diameter decreased. Because this anisotropic deformation was elastically recovered when the films were released, the change in resistivity was observed to recover in this strain region.

However, when the applied strain is larger, the change in the resistivity of the pristine films is caused by the coalescence of PEDOT-rich cores. The increase in core size caused by mechanical deformation is hardly recovered but is permanently maintained even after the films are completely released. Although the shrinkage occurs during the release of the films, the effect of the dimensional change on the cores size is small. For example, the core area decreased only 1% by the dimensional change during the release from 42% strain to the load-free state (28% strain). AFM analysis (Supporting Information Figure S4) shows that the core area is 2.85×10^{-2} μm for the sample of 42% strain. After the strain releasing, the core area is still maintained at 2.70×10^{-2} μm. The altered resistivity is also maintained over time, as shown in Supporting Information-Figure S5. Moreover, as shown in Figure 6b, the anisotropic-to-isotropic transition of the resistivity appears above 7% strain. In the AFM phase images (Figure 4b–d), the equivalent growth of the cores can be observed independent of the stretching direction. Beyond 7% strain, the slope of the change in resistivity in the perpendicular direction is nearly identical to that in the parallel direction. Therefore, the resistivity of the pristine films can be reduced permanently and isotropically because of the coalescence of the cores induced by large strain.

This isotropic and permanent nature of the electrical resistivity of PEDOT:PSS films induced by mechanical deformation provides another way in which the electrical properties of the films can be modulated. To date, only chemical doping has been used for such a purpose.

3. Conclusions

In this study, we investigated the change in the resistivity of pristine and DMSO-doped PEDOT:PSS as a function of tensile deformation. We obtained crack-free PEDOT:PSS stretchable conductors at a strain of 60% by using PI substrates, which have mechanical properties that are similar to those of PEDOT:PSS films. These results demonstrate that we can directly determine intrinsic changes in resistivity solely by studying morphological changes. The resistivity of DMSO-doped PEDOT:PSS films remains constant with respect to strain because conducting PEDOT chains are homogeneously dispersed and delocalized. In contrast, the resistivity of pristine PEDOT:PSS films was observed to decrease by up to 90%. This decrease is primarily caused by the unique morphological changes of the pristine PEDOT:PSS films. Stretching to large tensile strains gives rise to the unusual coalescence of conductive PEDOT-rich cores. An increase in core size is permanently maintained during stretching and even after releasing the films, which results in an irreversible decrease in resistivity. We conclude that tensile strain in PEDOT:PSS films significantly influences the morphological changes of the films and is dependent on the DMSO doping concentration. The resulting morphological changes directly lead to changes in electrical properties. According to these results, the resistivity of PEDOT:PSS films can be modulated to be negative with the application of tensile strain due to the permanent deformation of the films' morphology.

4. Experimental Section

Preparation of PEDOT:PSS Solution and Films: PEDOT:PSS (Clevios PH 1000, Heraeus) solutions with different concentrations (by weight) of dimethyl sulfoxide (DMSO) solvent (>99.9%, Sigma-Aldrich) as a doping material were prepared. The weight fractions of DMSO contained

in the PEDOT:PSS solution were 0, 5, and 10 wt%. The PEDOT:PSS/DMSO solutions were stirred for 24 h at room temperature in a N_2 glove box and filtered with polypropylene filters (0.45 μm pore size). The PEDOT:PSS films were formed by spin-coating at 1000 rpm for 30 s onto polyimide (PI) substrates (Kapton 300 HN, DuPont) treated with oxygen plasma (100 W, 75 mTorr O_2, 120 s by RIE 80 PLUS, Oxford Instrument) and onto PDMS (Sylgard 184, Base/Cross-linker = 10:1, Dow Corning) substrates under the same conditions. The spin-coated films were annealed on a hot plate for 15 min at 130 °C in a N_2 ambient glove box and then cooled to room temperature in the glove box. Subsequently, the PEDOT:PSS films cast on O_2-plasma-treated PI substrates and PDMS substrates were cut into rectangles measuring 10 mm in width and 30 mm in length.

Characterization of Electrical and Morphological Properties of PEDOT:PSS Films by Stretching/Releasing Tests: Uniaxial stretching tests were conducted on the PEDOT:PSS films by using a micro tensile machine (MMT-500N, Shimadzu) equipped with an electrically contactable jig for in situ resistance measurements (Figure 1). All tests were conducted at room temperature at a constant strain rate of 5×10^{-5} s^{-1}. As the films were deformed by uniaxial tension, the electrical resistance of the films was measured with an Agilent 34410A multimeter. The initial electrical conductivities of the films were measured using the four-point probe technique. Surface images of the PEDOT:PSS films were taken using an optical microscope and SEM (FE-SEM S-4800, Hitachi) at each strain. Atomic force microscope (AFM) phase images were obtained with a NANO Station II instrument operating in non-contact tapping mode under ambient conditions.

Supporting Information

Supporting Information is available from the Wiley Online Library or from the author.

Acknowledgements

This research was supported by the Converging Research Center Program through the Ministry of Education, Science and Technology (2012K001290). K.T.N. also appreciates the support from the Global Frontier R&D Program on Center for Multiscale Energy System funded by NRF (2011-0031574).

Received: December 12, 2012
Revised: January 29, 2013
Published online: March 15, 2013

[1] Y. M. Niquet, C. Delerue, C. Krzeminski, *Nano Lett.* **2012**, *12*, 3545.
[2] S. Chiu, J. Leu, P. Ho, *J. Appl. Phys.* **1994**, *76*, 5136.
[3] D. R. Cairns, R. P. Witte II, D. K. Sparacin, S. M. Sachsman, D. C. Paine, G. P. Crawford, R. Newton, *Appl. Phys. Lett.* **2000**, *76*, 1425.
[4] T. Li, Z. Huang, Z. Xi, S. P. Lacour, S. Wagner, Z. Suo, *Mech. Mater.* **2005**, *37*, 261.
[5] S. P. Lacour, D. Chan, S. Wagner, T. Li, Z. Suo, *Appl. Phys. Lett.* **2006**, *88*, 204103.
[6] N. Lu, X. Wang, Z. Suo, J. Vlassak, *Appl. Phys. Lett.* **2007**, *91*, 221909.
[7] B. Erdem Alaca, M. Saif, H. Sehitoglu, *Acta Mater.* **2002**, *50*, 1197.
[8] N. Cordero, J. Yoon, Z. Suo, *Appl. Phys. Lett.* **2007**, *90*, 111910.
[9] J. Y. Sun, N. Lu, J. Yoon, K. H. Oh, Z. Suo, J. J. Vlassak, *J. Mater. Res.* **2009**, *24*, 3338.
[10] T. Sekitani, Y. Noguchi, K. Hata, T. Fukushima, T. Aida, T. Someya, *Science* **2008**, *321*, 1468.
[11] K. Y. Chun, Y. Oh, J. Rho, J. H. Ahn, Y. J. Kim, H. R. Choi, S. Baik, *Nat. Nanotechnol.* **2010**, *5*, 853.
[12] Z. Yu, Q. Zhang, L. Li, Q. Chen, X. Niu, J. Liu, Q. Pei, *Adv. Mater.* **2011**, *23*, 664.
[13] T. Someya, T. Sekitani, S. Iba, Y. Kato, H. Kawaguchi, T. Sakurai, *Proc. Natl. Acad. Sci. USA* **2004**, *101*, 9966.
[14] D.-H. Kim, J. Song, W. M. Choi, H.-S. Kim, R.-H. Kim, Z. Liu, Y. Y. Huang, K.-C. Hwang, Y.-w. Zhang, J. A. Rogers, *Proc. Natl. Acad. Sci. USA* **2008**, *105*, 18675.
[15] J. A. Rogers, T. Someya, Y. Huang, *Science* **2010**, *327*, 1603.
[16] S. Kirchmeyer, K. Reuter, *J. Mater. Chem.* **2005**, *15*, 2077.
[17] Y. J. Lin, F. M. Yang, C. Y. Huang, W. Y. Chou, J. Chang, Y. C. Lien, *Appl. Phys. Lett.* **2007**, *91*, 092127.
[18] J. Huang, P. F. Miller, J. S. Wilson, A. J. De Mello, J. C. De Mello, D. D. C. Bradley, *Adv. Funct. Mater.* **2005**, *15*, 290.
[19] S. Ghosh, O. Inganäs, *Synth. Met.* **2001**, *121*, 1321.
[20] J. Y. Kim, J. H. Jung, D. E. Lee, J. Joo, *Synth. Met.* **2002**, *126*, 311.
[21] X. Crispin, S. Marciniak, W. Osikowicz, G. Zotti, A. W. D. van der Gon, F. Louwet, M. Fahlman, L. Groenendaal, F. De Schryver, W. R. Salaneck, *J. Polym. Sci. Pol. Phys.* **2003**, *41*, 2561.
[22] S. K. M. Jönsson, J. Birgerson, X. Crispin, G. Greczynski, W. Osikowicz, A. W. Denier van derGon, W. R. Salaneck, M. Fahlman, *Synth. Met.* **2003**, *139*, 1.
[23] J. Ouyang, Q. Xu, C. W. Chu, Y. Yang, G. Li, J. Shinar, *Polymer* **2004**, *45*, 8443.
[24] S. Timpanaro, M. Kemerink, F. J. Touwslager, M. M. De Kok, S. Schrader, *Chem. Phys. Lett.* **2004**, *394*, 339.
[25] G. Latessa, F. Brunetti, A. Reale, G. Saggio, A. Di Carlo, *Sens. Actuators B.* **2009**, *139*, 304.
[26] S. Takamatsu, T. Takahata, M. Muraki, E. Iwase, K. Matsumoto, I. Shimoyama, *J. Micromech. Microeng.* **2010**, *20*.
[27] D. J. Lipomi, J. A. Lee, M. Vosgueritchian, B. C. K. Tee, J. A. Bolander, Z. Bao, *Chem. Mater.* **2011**, *24*, 373.
[28] V. Vijay, A. D. Rao, K. S. Narayan, *J. Appl. Phys.* **2011**, *109*.
[29] U. Lang, N. Naujoks, J. Dual, *Synth. Met.* **2009**, *159*, 473.
[30] S. J. Clarson, J. A. Semlyen, S. J. Clarson, *Siloxane Polymers*, Prentice Hall Englewood Cliffs, New Jersey **1993**.
[31] H. Hillborg, J. Ankner, U. W. Gedde, G. Smith, H. Yasuda, K. Wikström, *Polymer* **2000**, *41*, 6851.
[32] K. Efimenko, W. E. Wallace, J. Genzer, *J. Colloid Interface Sci.* **2002**, *254*, 306.
[33] P. Gorrn, S. Wagner, *J. Appl. Phys.* **2010**, *108*, 093522.
[34] D. Y. W. Yu, F. Spaepen, *J. Appl. Phys.* **2004**, *95*, 2991.
[35] A. Aleshin, S. Williams, A. Heeger, *Synth. Met.* **1998**, *94*, 173.
[36] A. M. Nardes, R. A. J. Janssen, M. Kemerink, *Adv. Funct. Mater.* **2008**, *18*, 865.
[37] R. Jalili, J. M. Razal, P. C. Innis, G. G. Wallace, *Adv. Funct. Mater.* **2011**, *21*, 3363.
[38] J. H. Huang, D. Kekuda, C. W. Chu, K. C. Ho, *J. Mater. Chem.* **2009**, *19*, 3704.
[39] U. Lang, E. Müller, N. Naujoks, J. Dual, *Adv. Funct. Mater.* **2009**, *19*, 1215.
[40] D. Tahk, H. H. Lee, D.-Y. Khang, *Macromolecules* **2009**, *42*, 7079.
[41] A. Nardes, M. Kemerink, R. Janssen, *Phys. Rev. B* **2007**, *76*, 085208.
[42] N. Mott, E. A. Davis, in *Electronic Processes in Non-Crystalline Materials*, Clarendon Press, Oxford **1979**.
[43] Y. Cao, P. Smith, A. J. Heeger, *Polymer* **1991**, *32*, 1210.
[44] A. Monkman, P. Adams, *Synth. Met.* **1991**, *40*, 87.